

A dark blue vertical bar on the left side of the page. A blue arrow points to the right from the bar, containing the date.

23.04.2018

Motor Winding Design & Analysis

EE564 – Project 2

Several thin, curved lines in dark blue and light grey originate from the bottom left and curve upwards and to the right.

Furkan KARAKAYA
1937051

Content

1) INTRODUCTION	2
2) WINDING DESIGN	2
3) MOTOR PARAMETER ESTIMATION	6
4) DETAILED ANALYSIS & VERIFICATION	8
5) CONCLUSION	13

1) INTRODUCTION

In this project, an asynchronous machine is designed by applying analytical methods and the results are verified using finite element analysis program. For this purpose, after selecting the lamination, the winding design is performed. Critical parameters like pole number, phase number, type of winding, number of turns etc. are chosen. Then for the selected parameters the performance of the induction motor is studied. Finally, the results are verified using finite element analysis computer program.

2) WINDING DESIGN

The induction motor is designed using the first lamination¹ given in the list. The parameters of this lamination are given in Table 1 and also the figure 1 shows the 2D drawing of the lamination.

Stator Outer Diameter	170 mm
Stator Inner Diameter	115 mm
Rotor Outer Diameter	114.6 mm
Rotor Inner Diameter	45 mm
Stator Slot Number	36
Rotor Slot Number	33
Stator Slot Area	93.3 mm ²
Rotor Slot Area	47.5 mm ²

Table 1: The specs of Lamination 1

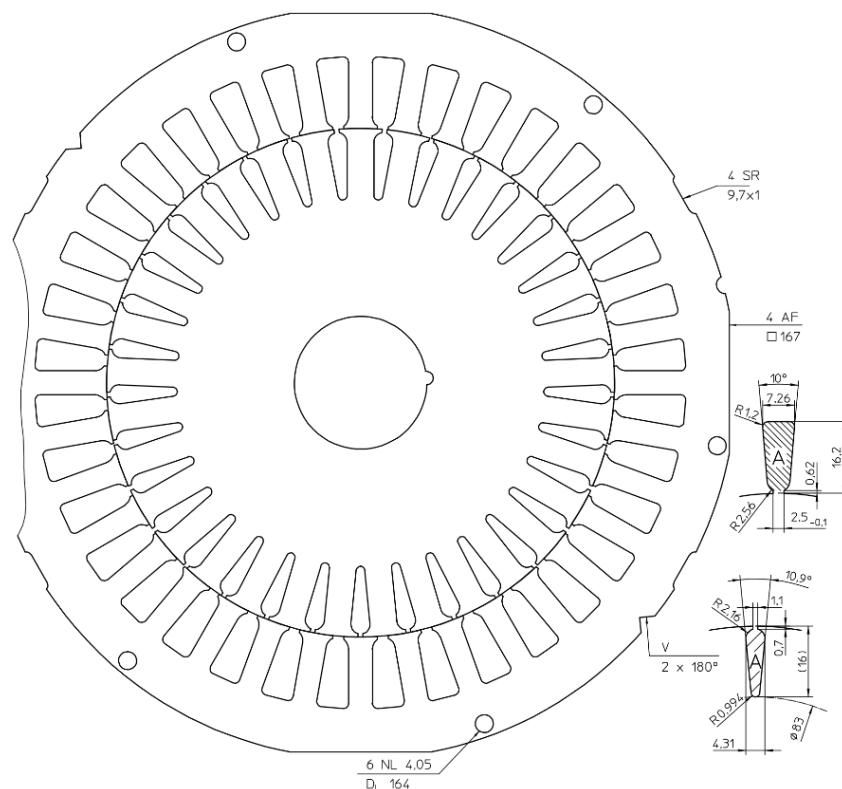


Figure 1: The 2D drawing of the Lamination 1

¹ [https://github.com/odtu/ee564-2018/blob/master/Project2/ks\(1\).pdf](https://github.com/odtu/ee564-2018/blob/master/Project2/ks(1).pdf)

In order to evaluate the performance of the induction motor, it is required to decide critical design parameters. Table 2 shows the selected main parameters of the studied design.

Phase Number	3
Pole Number	4
Connection	wye
Line Voltage	380 Vrms
Frequency	50 Hz

Table 2: Selected Main Parameters

$$q = \frac{Q}{2pm} = \frac{36}{2 * 2 * 3} = 3 \quad (1)$$

As shown in equation 1, q is equal to 3 which is an integer number therefore the design is performed for integral, single layer type of winding. The resulting winding diagram of the design is given in Table 3.

1	2	3	4	5	6	7	8	9	10	11	12	13	14	15	16	17	18
A	A	A	-B	-B	-B	C	C	C	-A	-A	-A	B	B	B	-C	-C	-C

Table 3: Winding Diagram for Single Layer Integral Type of Winding

For this winding scheme, the MMF is plotted for three different case where the turn number is taken as one and the current peak value is also taken as one. Therefore, to calculate the actual MMF value, just the extension with NI coefficient is enough. The MMF plots of the cases are shown in Figure 2, 3 and 4. In both plots, the MMF is given for 18 slots which covers a pole pair. Thus, the plots just repeat itself for each pole pair.

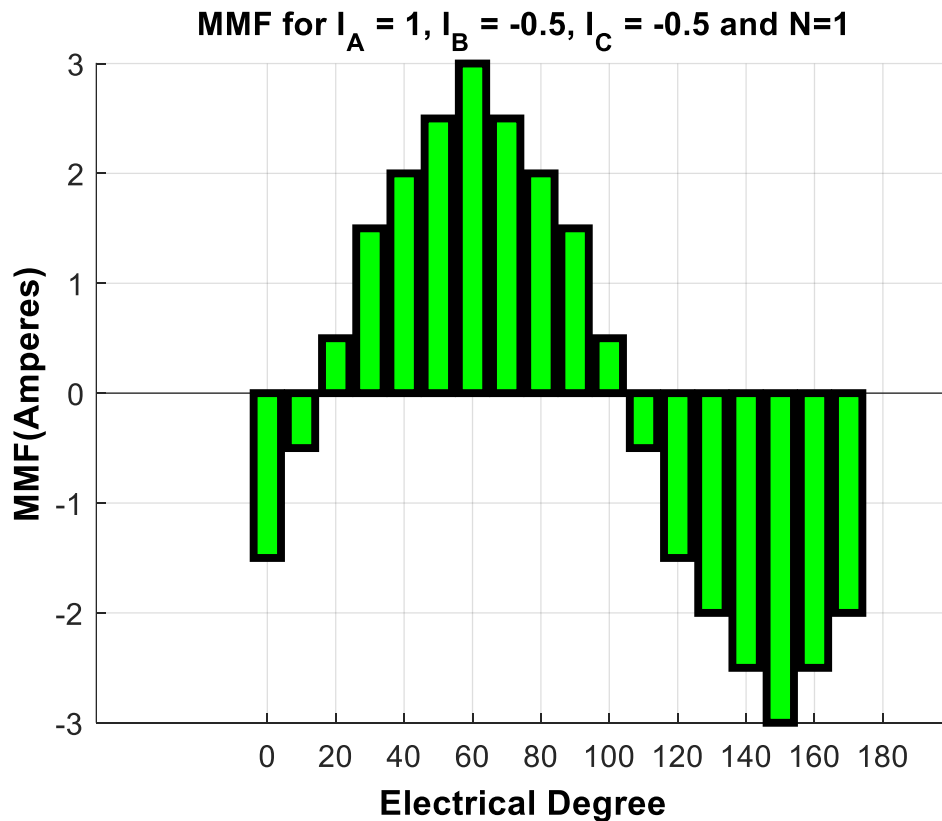


Figure 2: MMF plot for $I_a = 1$ and $I_b = I_c = -0.5$

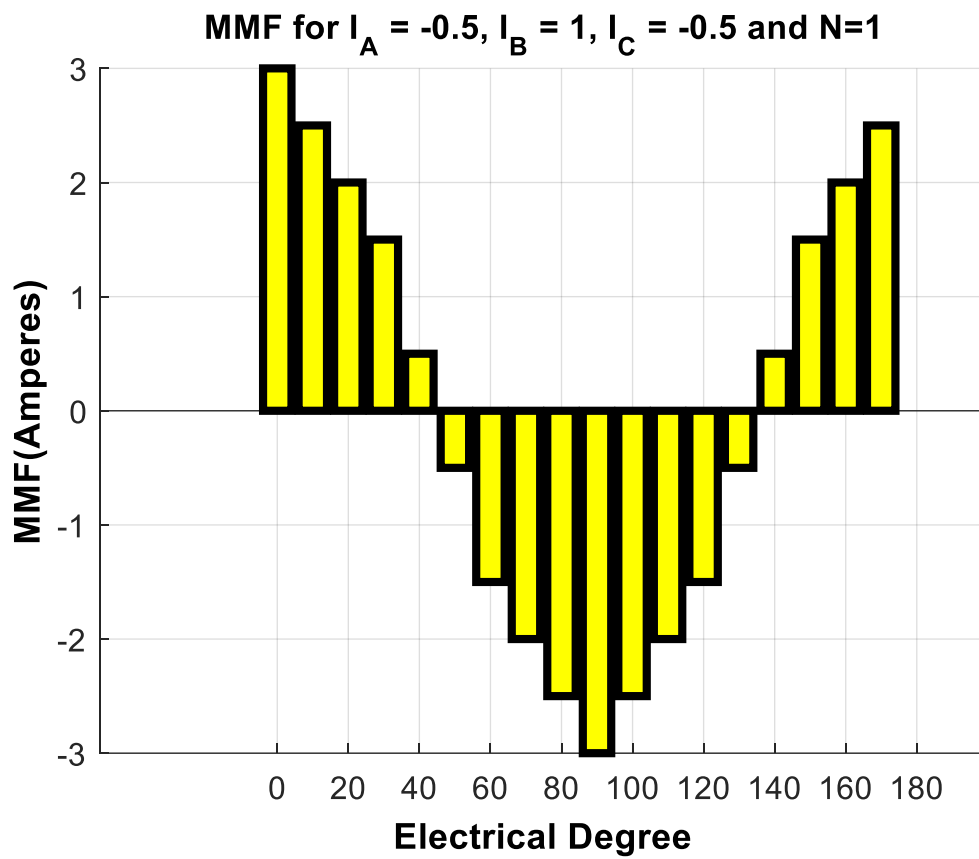


Figure 3: MMF plot for $I_b = 1$ and $I_a = I_c = -0.5$

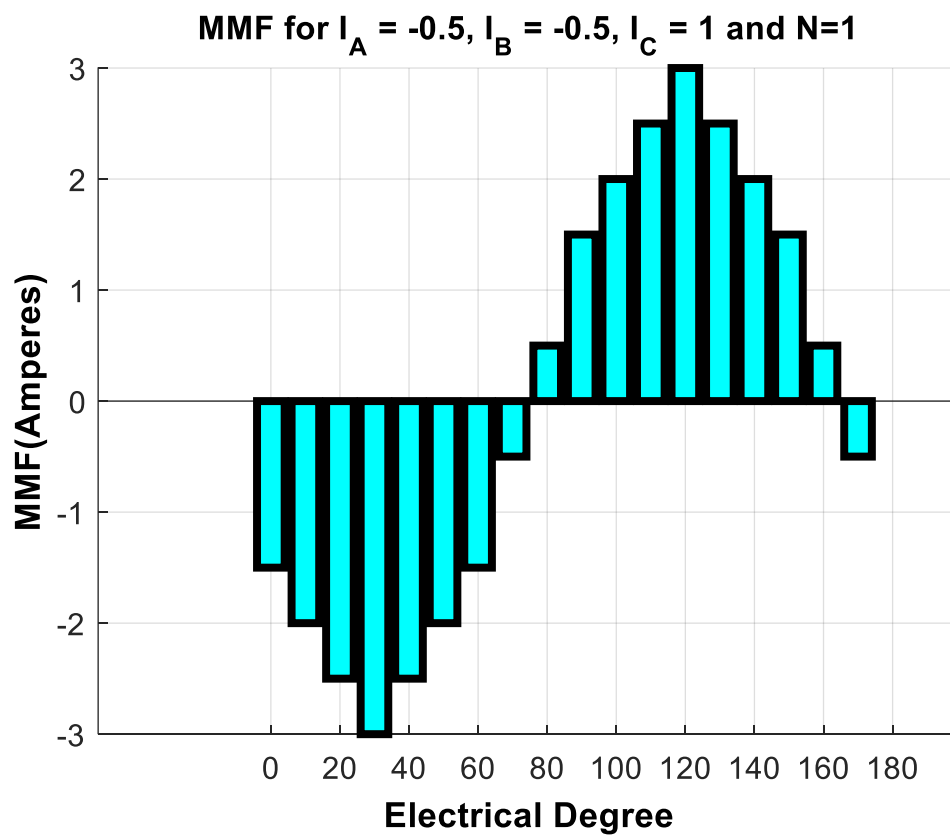


Figure 4: MMF plot for $I_c = 1$ and $I_b = I_a = -0.5$

Then, in order to calculate the winding factor of this winding, the pitch factor and distribution factor should be calculated. The calculations are done using the eqn. (2) and (3). The coil pitch in electrical degrees, λ , is 180° for the first harmonic because this is a full-pitch machine. Also the electrical angle between each coil, α , is 20° because a pole pair has 18 slots which is 360° in total. After calculating the pitch factor and distribution factor, the winding factor is calculated for each harmonic by multiplying the pitch factor and distribution factor as given in eqn. (4). The results are also given in Table 4.

$$k_p(n) = \sin\left(n \frac{\lambda}{2}\right) \quad (2)$$

$$k_d(n) = \frac{\sin\left(\frac{qn\alpha}{2}\right)}{q \sin\left(\frac{n\alpha}{2}\right)} \quad (3)$$

$$k_w(n) = k_p(n) * k_d(n) \quad (4)$$

Harmonic Order	Pitch Factor	Distribution Factor	Winding Factor
1	1	0.9598	0.9598
2	0	0.8440	0
3	-1	0.6667	-0.6667
4	0	0.4491	0
5	1	0.2176	0.2176
6	0	0	0
7	-1	-0.1774	0.1774
8	0	-0.2931	0
9	1	-0.3333	-0.3333
10	0	-0.2931	0
11	-1	-0.1774	0.1774

Table 4: Pitch Factor, Distribution Factor and Winding Factor Values for first 11 harmonics

Note that, since this is a three phase induction machine, the integer multiples of third harmonic will be eliminated for line observations. Having decided the main parameters and connection type of the motor the axial length of the stator & rotor is calculated with the consideration of the aspect ratio. Even though, the typical aspect ratio of the induction motor is close to 1, eqn. (5), the axial length is selected as 150mm to produce higher torque. Also the length of the air gap is calculated as 0.188 mm, eqn. (6), in order to satisfy the manufacturing clearance, it is taken as 0.2 mm.

$$\chi = \frac{D}{L} = \frac{\pi}{2p} * \sqrt[3]{p} = 0.989 \quad (5)$$

$$\delta = 0.18 + 0.006 * P^{0.4} \quad (6)$$

Decision of the axial length is important for choosing the turns number because it changes the pole area. The turn number of phase is calculated using eqn. (8) where the pole area is calculated with respect to the eqn. (7). Note that, the phase voltage of the electrical motor, 220V, is multiplied with 0.9 to take the voltage drop into account.

$$A_{pole} = \frac{\pi * D}{2p} * L \quad (7)$$

$$N_{phase} = \frac{E_{rms} * 0.9}{4.44 * f * k_{w1} * B_{avg} * A_{pole}} \quad (8)$$

The peak value of the flux density of the air gap over a pole is taken as 0.4 T which means having an average value around 0.25 T. Actually, in literature the peak value of the flux density is given as 0.7T – 0.9T; however, in finite element analysis it is observed the yoke of the stator is saturated for this level of flux density, so it is reduced to 0.4 T so as to decrease the losses.

After calculating the turn number of phase, the conductor number per slot is calculated using eqn. (9) which gives 45 conductors. Therefore, having decided the number of conductors per slot the wire diameter can be calculated using eqn. (10). The fill factor is selected as 0.75 which is actually a bit tighter. For this calculation the diameter of wire can be increased up to 1.407 mm.

$$N_{slot} = \frac{N_{phase}}{q * p} = 45 \quad (9)$$

$$N_{slot} * \pi * \left(\frac{D_{wire}}{2}\right)^2 = FF * A_{slot} \quad (10)$$

3) MOTOR PARAMETER ESTIMATION

Up to now, the main parameters of the electrical machine is selected. In this part, the performance related parameters will be calculated and decided. Since the turn number is known, the stator current can be calculated using the electrical loading. In asynchronous machines, electrical loading can be in between 30-65 kA/m. In this design, the peak value of the electrical loading is selected as 38 kA/m. Therefore, the RMS value of the electrical loading is 26.87 kA_{RMS}/m. Using the eqn. (11), the RMS value of the stator current is calculated as 6 A_{RMS}.

$$A_{RMS} = \frac{Q * N_{slot} * I_{stator}}{\pi * D} \quad (11)$$

Since both the line voltage and line current is known now, the input apparent power can be calculated easily using eqn. (12). For a proper design, the power factor and efficiency should be high as possible as. Thus, in this design PF is taken as 0.9 and efficiency is considered as 0.85. As calculated in eqn. (13), corresponding output power is 3025 W, nearly 3 kW.

$$S_{in} = \sqrt{3} * V_{line} * I_{stator} \quad (12)$$

$$P_{out} = S_{in} * PF * Efficiency \quad (13)$$

Furthermore, the magnetic loading is actually decided before because the magnetic loading is nothing but the average air-gap flux density over a pole. The peak value of the magnetic loading is taken as 0.4 T. As a result, since both the magnetic loading and electrical loading are known, the tangential stress on the rotor can be calculated which will draw us to the rated output torque. The tangential stress is calculated using eqn. (14) and the rated torque is calculated in eqn. (15). Therefore, the stress is 6840 Pa and rated torque is 21.3 Nm.

$$\sigma_{tan} = \frac{A_{rms} * \hat{B} * PF}{\sqrt{2}} \quad (14)$$

$$T_{out} = 2 * \sigma_{tan} * V_r \quad (15)$$

As a last indicator of performance, the slip can be calculated as well. The following eqns. clearly describe the calculation.

$$\omega_{shaft} = \frac{P_{out}}{T_{out}} \quad (16)$$

$$n_{synch} = \frac{120 * f}{2 * p} = 1500 \text{ rpm} \quad (17)$$

$$n_{shaft} = \omega_{shaft} * \frac{30}{\pi} = 1355 \text{ rpm} \quad (18)$$

$$s = \frac{n_{synch} - n_{shaft}}{n_{synch}} = 0.096 \quad (19)$$

The equivalent resistance of the stator and rotor is calculated for 75 °C. It is assumed that stator and rotor have the same phase resistances. So, firstly, the resistivity of copper for 75 °C is calculated using eqn. (20) where resistivity for 20 °C is 1.68e-8 and α is 0.0038. Then the phase resistance is calculated for the stator.

$$\rho_{75}(\text{ohm-meter}) = (1 + \alpha * (75 - 20)) * \rho_{20^\circ C} \quad (20)$$

$$R_{phase} = N_{phase} * \rho_{75} * \frac{2 * (L + \pi * \frac{D}{4})}{A_{wire}} = 1.69 \Omega \quad (21)$$

The mutual inductance is an important factor which determines the power factor of the electrical machine. In this design, it is calculated using eqn. (22)². The mutual inductance is important for the power factor estimation. Low mutual inductances result in higher magnetizing current which definitely reduces the power factor. The resulting mutual inductance is calculated as 450mH which has 141-ohm magnetizing branch impedance.

$$L_m = \frac{m}{\pi} * \frac{\mu_0}{\delta} * D * L * \left(\frac{N_{phase}}{2p} \right)^2 * k_{w1} \quad (22)$$

Then the leakage inductances are calculated using the following eqns. (23) – (27). The equations are taken from the lecture book. In eqn. (23), the coefficient for stator leakage inductance is calculated. As seen, the harmonics other than the first one contributes to the leakage while the main components results in the mutual inductance. For the rotor side, in eqn. (25) the skewing factor is calculated where each bar shifts one slot on the rotor. Then, in eqn. (26), the coefficient for rotor leakage inductance is calculated to find out the inductance referred to stator side, eqn. (27).

$$\sigma_\delta = \sum_{i=2}^{11} \left(\frac{k_{wi}}{i * k_{w1}} \right)^2 = 0.0581 \quad (23)$$

$$L_{leak-stator} = \sigma_\delta * L_m = 26.1 \text{ mH} \quad (24)$$

$$k_{sq} = \frac{\sin\left(\frac{\pi}{2} * \frac{1}{m * q}\right)}{\frac{\pi}{2} * \frac{1}{m * q}} = 0.995 \quad (25)$$

$$\sigma_{\delta r} = \frac{1}{k_{sq}^2} * \left(\frac{p * \frac{\pi}{Q_r}}{\sin\left(p * \frac{\pi}{Q_r}\right)} \right)^2 - 1 = 0.0225 \quad (26)$$

$$L'_{\delta r} = \sigma_{\delta r} * L_m = 10.1 \text{ mH} \quad (27)$$

² Nerg, J., Partanen, J., & Ritchie, E. (2004). Induction Motor Magnetizing Inductance Modelling as a Function of Torque, 40(4), 2047–2049.

For the calculated parameters now, the losses can be calculated roughly. Assuming the magnetizing current is nearly zero, so the stator current is equal to rotor current, the eqn. (28) gives the copper loss.

$$P_{copper-loss} = 2 * R_{phase} * I_{stator}^2 = 360 W \quad (28)$$

For the selected material, *JFE_Steel_20JNEH1500*, the core loss is calculated using the following formula, eqn. (29). Where the K_h is 176.3, K_c is 0.102 and K_e is 2.724 and B_m is taken as 1 Tesla. Since V_{stator} is $2.784 \times 10^{-3} m^3$, the core loss is calculated as 28W.

$$P_{core} = V_{stator} * [K_h * f * (B_m)^2 + K_c * (f * B_m)^2 + K_e * (f * B_m)^{1.5}] = 28W \quad (29)$$

4) DETAILED ANALYSIS & VERIFICATION

The finite element analysis is conducted on RMxpert. The stator winding scheme is given in the next Figure 5, which is the same of the designed.

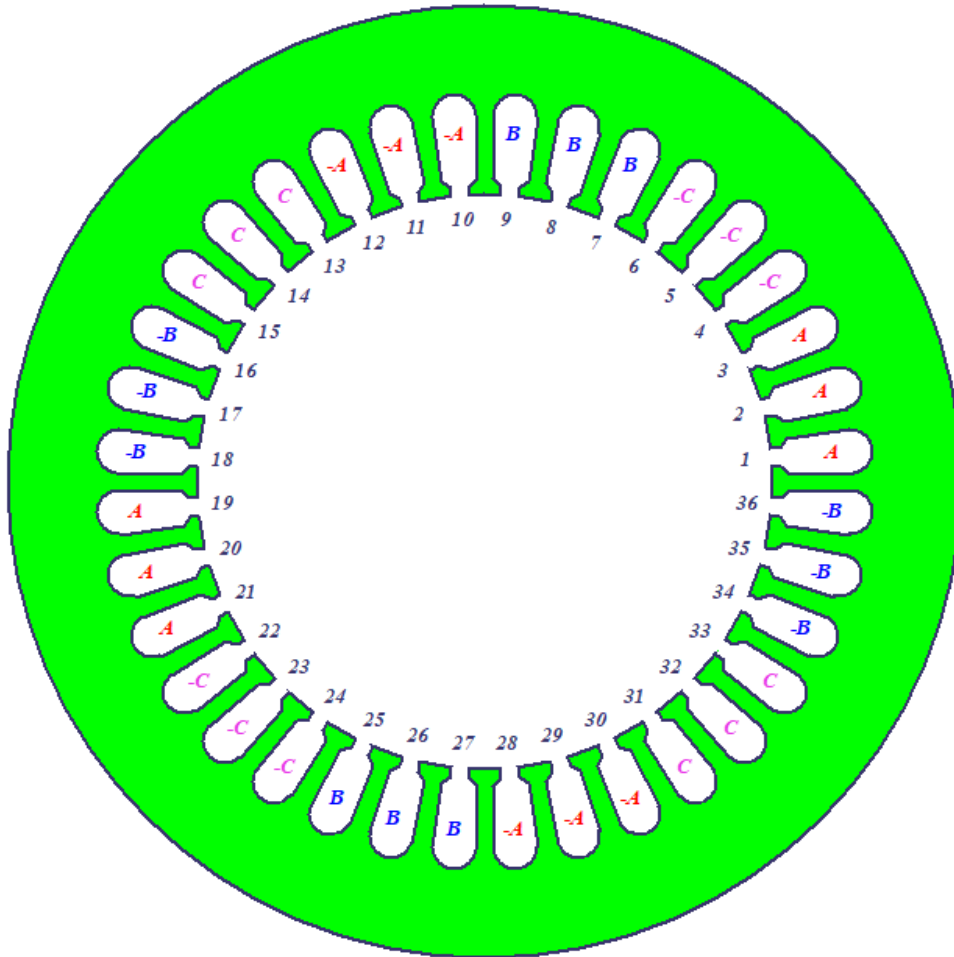


Figure 5: The winding scheme of the stator in RMxpert

Now, in the following Table 5, the results are compared. The green color is used for the good results, while yellow for the moderate ones and grey for the bad results. As seen, in Table 5, the electrical loading and magnetic loading are quite closer which is good. Therefore, with small error the torque calculation is also okay. Those results might be much closer if the power factor is close better because it directly affects the output power and torque calculations. Even though the resistance values are

calculated wrongly, they might be considered as acceptable. However, the reactance calculations are absolutely wrong.

	Analytical Result	RMxpert Result
Electric Loading (Arms)	26870	27012
Magnetic Loading (Bpeak)	0.4	0.387
Power Factor	0.9	0.87
Efficiency	0.85	0.86
Output Power (W)	3025	3025
Shaft Torque (Nm)	21.3	20.5
Shaft Speed (rpm)	1355	1409
Stator Current (Arms)	6	6.02
Stator Phase Resistance (ohm)	1.69	2.03
Rotor Phase Resistance (ohm)	1.69	1.93
Mutual Reactance (ohm)	141	352
Stator Leak. Reactance (ohm)	8.2	5.95
Rotor Leak. Reactance (ohm)	3.18	9.45
Copper Loss (W)	362	415
Core Loss (W)	28	28.7

Table 5: Comparison Table

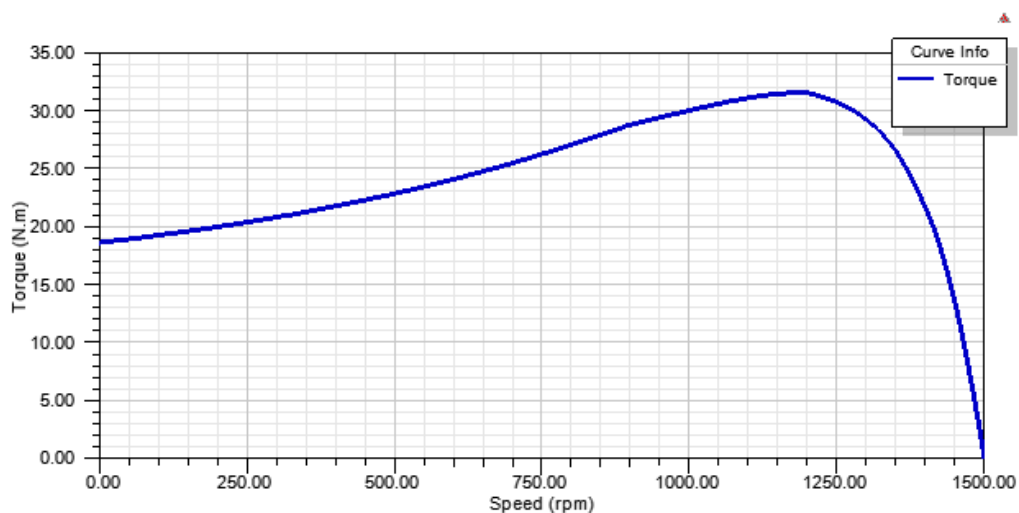


Figure 6: Torque-Speed Curve Graph

Figure 6 shows the torque speed graph. The operating condition of the motor can be selected using this figure. Also, in Figure 7, it is seen that the motor is fine if it is used 400W-3200W range. For other power values the efficiency decreases which is not deserved. Plus, Figure 8 shows that the motor has different efficiency values for different speeds so operating at appropriate speed is important for minimizing losses. Lastly, Figure 9 is helpful to estimate the inrush current because each motor when it starts rotating draws high amount of current and the driver electronics should be compatible with this current.

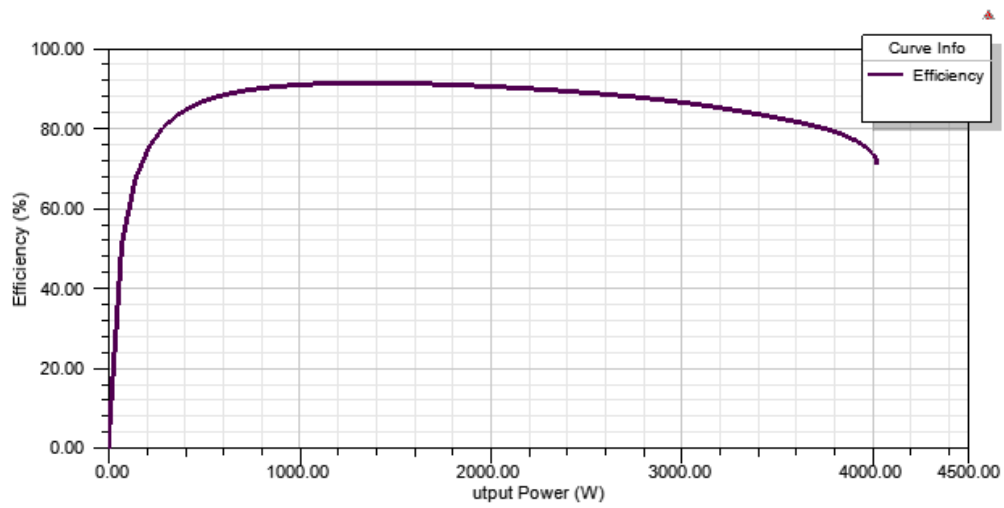


Figure 7: Efficiency vs Output Power

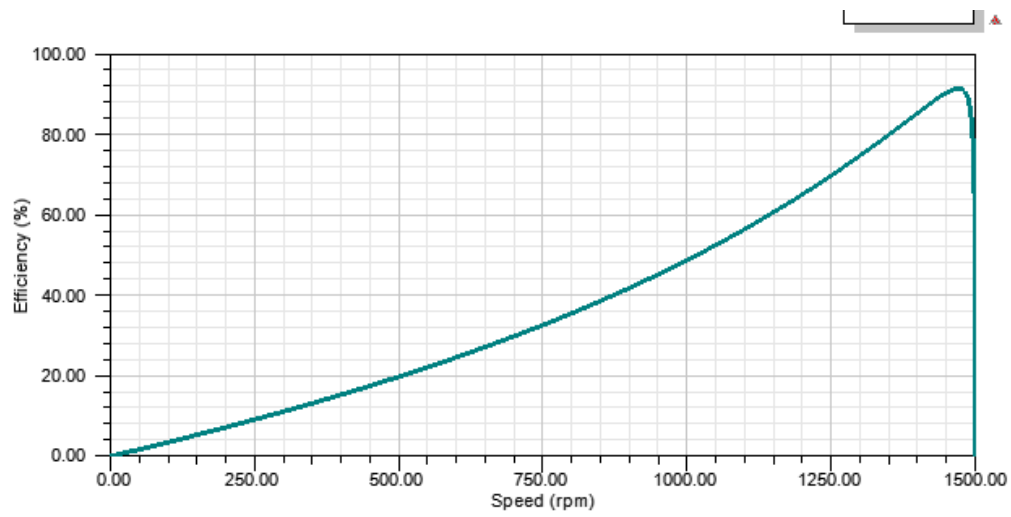


Figure 8: Efficiency vs Speed Graph

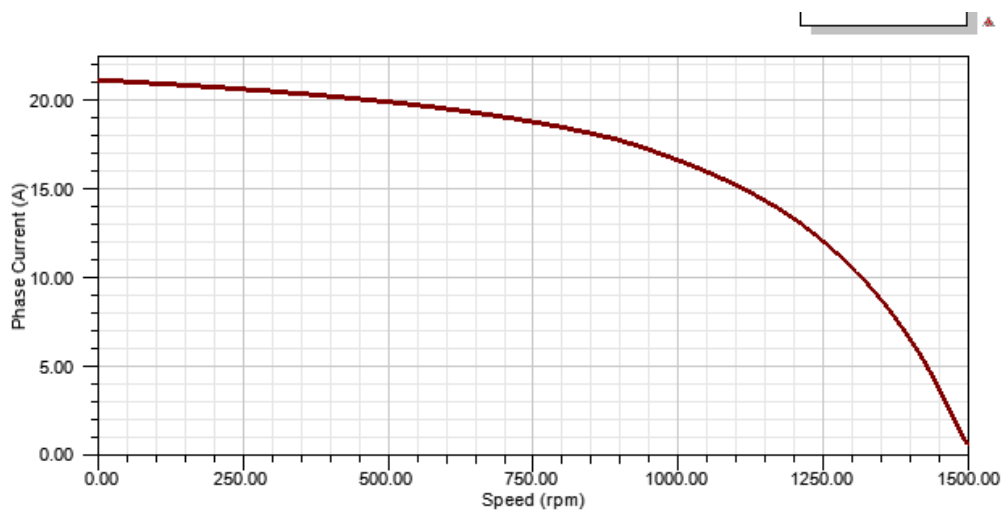


Figure 9: Phase Current vs Speed Graph

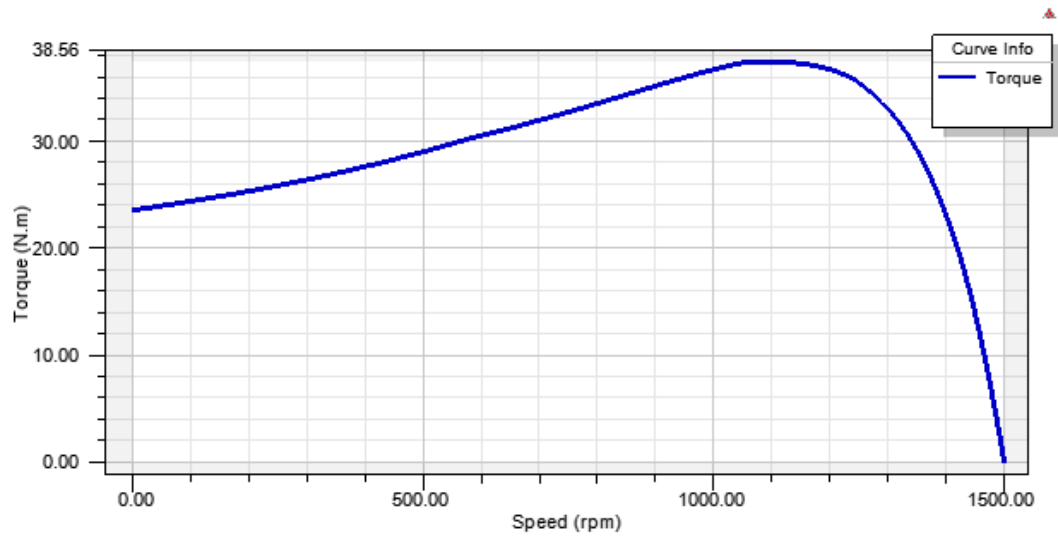


Figure 10: Torque vs Speed Graph when the skewing is cancelled

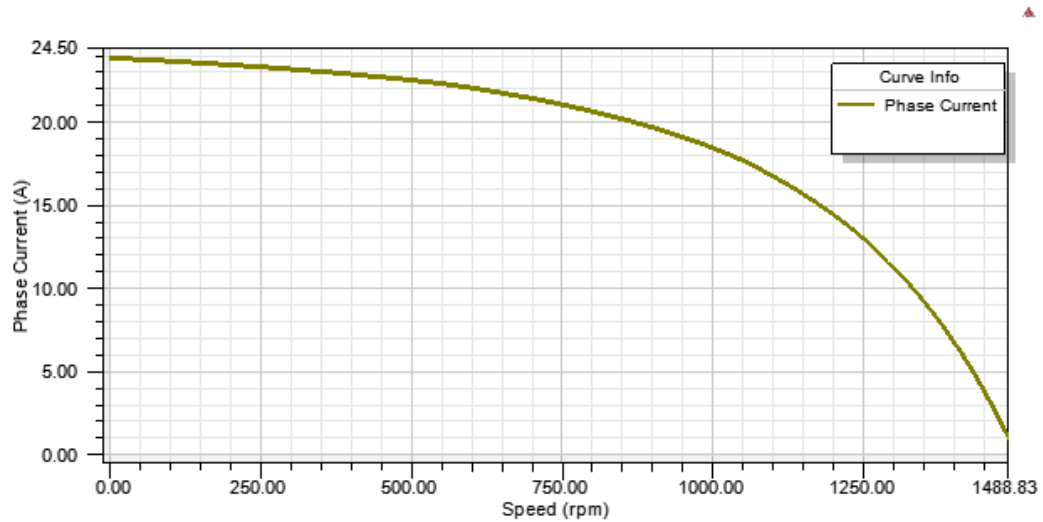


Figure 11: Phase Current vs Speed Graph when skewing is cancelled.

Comparing the Figure 10 and Figure 6 & Figure 11 and Figure 9, it is seen that when the skewing does not exist, the starting torque is higher than the skewed version because basically the cogging torque is much higher. Therefore, the inrush current is higher so it increases also the losses. Therefore, in order to increase the performance of the induction motor skewing should be applied.

In Figure 12, stator phase currents are given in steady state. Since the step time is taken high, their shape is distorted; however, they are clear enough to show the main component behaviour. It is weird to have this figure as a rated because its RMS value is much higher than the calculated one.

In Figure 13 and Figure 14, the flux density distribution over the motor are given for just the beginning moment of the acceleration and steady state condition. For the initial moment, since the current is not high as much as rated one, the flux density is lower but the poles are very visible. For the rated conditions, we observe the flux density is higher; however, it is seen that the yoke flux density is around 1.2T and tooth flux density is 1.6T at maximum value; therefore, the operation can be considered safe as desired.

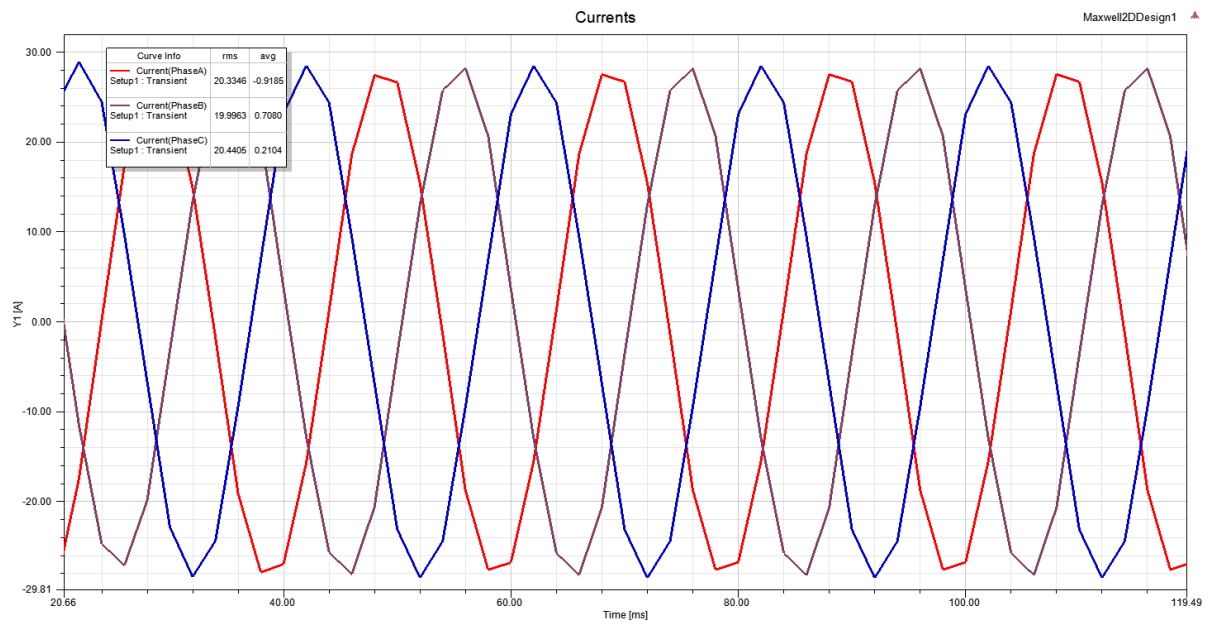


Figure 12: Stator Phase Currents

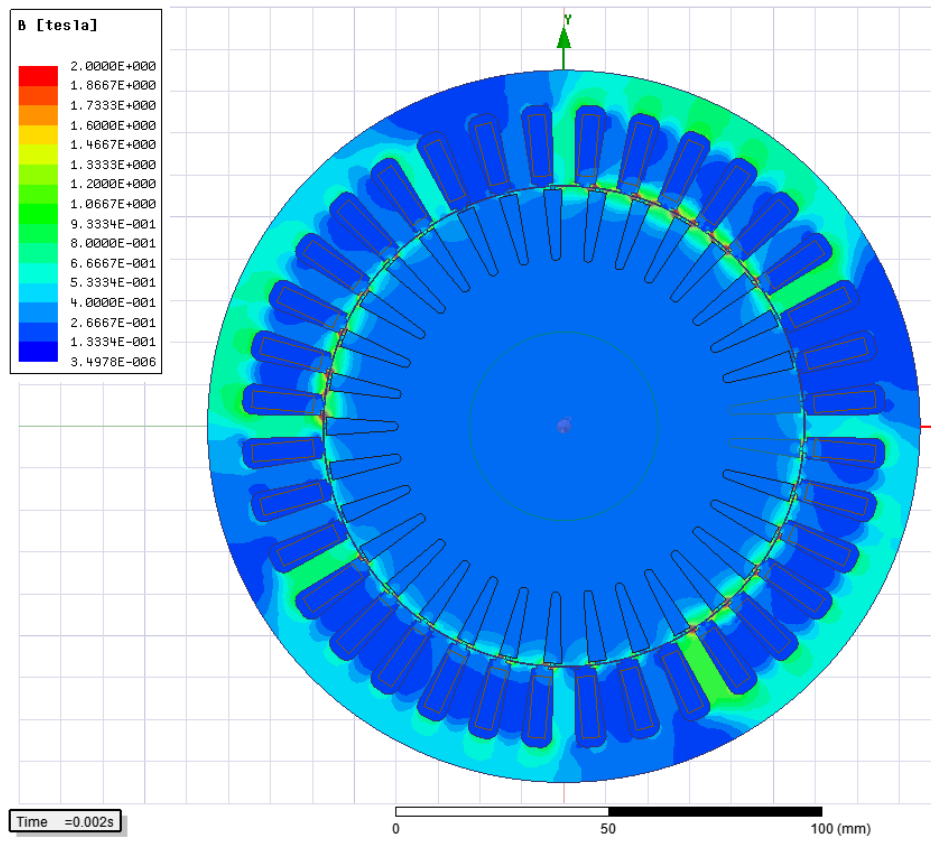


Figure 13: Flux Density Distribution Over the Motor (starting moment)

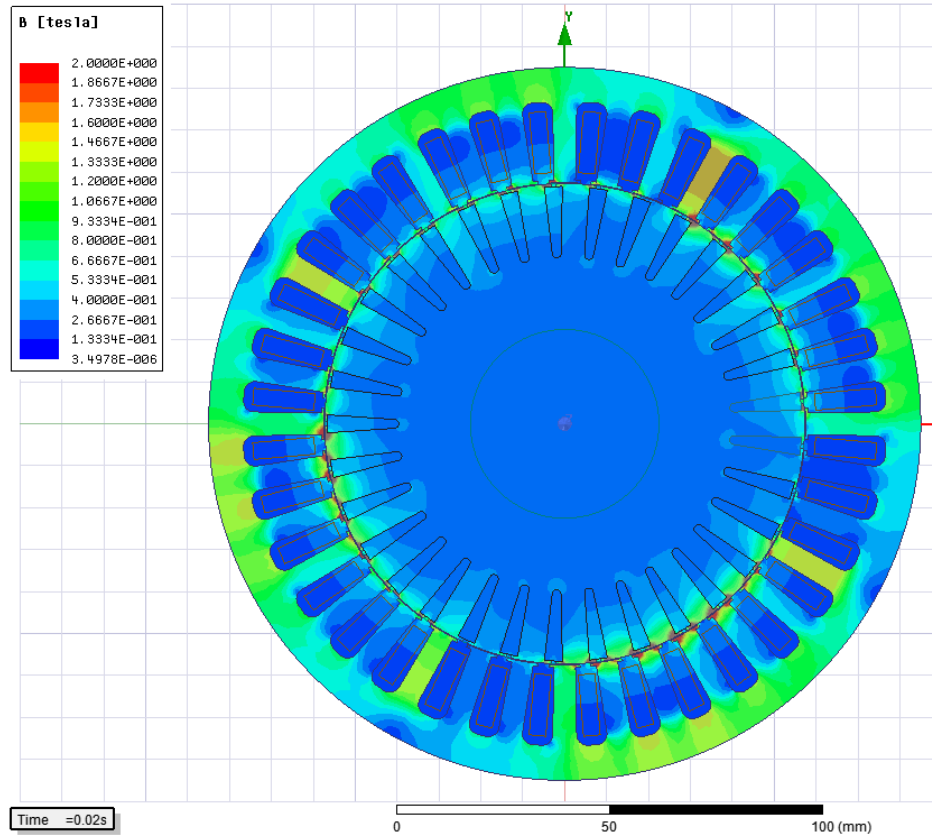


Figure 14: Flux Density Distribution Over the Motor (steady-state)

5) CONCLUSION

In this project, a three phase asynchronous motor whose output power is 3kW and rated torque is 20.2Nm is designed for the 115 mm bore diameter and 150 mm axial length. For this purpose, the lamination is selected and type of winding is decided. Having decided the windings, the MMF plots are obtained and analytical calculations are performed to evaluate performance and parameters of the induction motor. Then, the motor is analysed using a finite element analysis program and results are compared. It is seen that the electric and magnetic loading are verified with both analysis and the efficiency and power factor are closer to expected results. There are variations in the phase mutual and leakage inductances.

Moreover, efficiency-speed, torque-speed, efficiency-output power and current-speed graph are investigated to analyse motor performance and also see the effects of skewing on the squirrel cage rotor. It is seen that if the skewing is not applied the cogging torque increases and it results in higher amount of inrush current which is not desired. Lastly, the magnetic flux density plots are shared for the beginning and steady state moments and it is verified that the magnetic operation is performed without saturation on teeth and yoke except the teeth's edges.